Received: 2 May 2023 | Revised: 20 July 2023 | Accepted: 25 July 2023

DOI: 10.1002/dvdy.646

PHENOTYPE REPORT

Developmental Dynamics WILEY

Identification and characterization of *Hand2* upstream genomic enhancers active in developing stomach and limbs

Chloe A. Ferguson[1] | **Beth A. Firulli**[1] | **Matteo Zoia**[2] | **Marco Osterwalder**[2,3] | **Anthony B. Firulli**[1]

[1]Herman B Wells Center for Pediatric Research, Department of Pediatrics, Anatomy, Biochemistry, and Medical and Molecular Genetics, Indiana University School of Medicine, Indianapolis, Indiana, USA

[2]Department for BioMedical Research (DBMR), University of Bern, Bern, Switzerland

[3]Department of Cardiology, Bern University Hospital, Bern, Switzerland

Correspondence
Marco Osterwalder, Department for BioMedical Research (DBMR), University of Bern, 300, Bern, Switzerland.
Email: marco.osterwalder@unibe.ch

Anthony B. Firulli, Herman B Wells Center for Pediatric Research, Department of Pediatrics, Anatomy, Biochemistry, and Medical and Molecular Genetics, Indiana University School of Medicine, 1044 W. Walnut St., Indianapolis, Indiana 46202-5225, USA.
Email: tfirulli@iu.edu

Funding information
National Institutes of Health, Grant/Award Numbers: 1R01DE02909, 2P01HL134599, R01HL145060, R01HL120920; Swiss National Science Foundation, Grant/Award Number: PCEFP3_186993

Abstract

Background: The bHLH transcription factor HAND2 plays important roles in the development of the embryonic heart, face, limbs, and sympathetic and enteric nervous systems. To define how and when HAND2 regulates these developmental systems, requires understanding the transcriptional regulation of *Hand2*.

Results: Remarkably, *Hand2* is flanked by an extensive upstream gene desert containing a potentially diverse enhancer landscape. Here, we screened the regulatory interval 200 kb proximal to *Hand2* for putative enhancers using evolutionary conservation and histone marks in *Hand2*-expressing tissues. H3K27ac signatures across embryonic tissues pointed to only two putative enhancer regions showing deep sequence conservation. Assessment of the transcriptional enhancer potential of these elements using transgenic reporter lines uncovered distinct in vivo enhancer activities in embryonic stomach and limb mesenchyme, respectively. Activity of the identified stomach enhancer was restricted to the developing antrum and showed expression within the smooth muscle and enteric neurons. Surprisingly, the activity pattern of the limb enhancer did not overlap *Hand2* mRNA but consistently yielded a defined subectodermal anterior expression pattern within multiple transgenic lines.

Conclusions: Together, these results start to uncover the diverse regulatory potential inherent to the *Hand2* upstream regulatory interval.

KEYWORDS

embryonic development, hand factors, transcription

1 | INTRODUCTION

Embryogenesis is a structurally complex process that is dependent on spatiotemporal regulation of differentiation and growth within multiple diverse cell types that interweave to coordinate the formation of the viable embryo.[1,2] This process is composed of finely tuned gene regulatory networks with interactions of transcription factors and other regulatory layers that implement the cell programs, allowing for tissue differentiation.[3–6] Evolutionarily Conserved Non-Coding Sequences (CNSs) often include *cis*-regulatory elements that allow these CNS to act as transcriptional enhancers.[6] Thus, to gain an understanding of how genes fit into the required regulatory networks that drive embryogenesis, the identification of transcriptional

enhancers is a well-established strategy to reveal the details of these networks.[7–13]

The basic-Helix–Loop–Helix (bHLH) super-family of transcription factors are evolutionarily conserved and play a substantial role in regulating growth, development, and differentiation in many tissues during embryonic development.[14,15] Members of the TWIST family of bHLH transcription factors are particularly interesting since family members can function as either hetero or homodimers by binding to E-box (CANNTG) and D-box (CGNNTG) *cis*-elements in a variety of developing embryonic tissues.[14,16–18] The TWIST family member, HAND2 plays a crucial developmental role within the heart, limbs, neural crest, craniofacial and the sympathetic nervous system (SNS).[19–25] Previous studies have demonstrated that both loss- and gain-of function mutations of *Hand2* have led to various severe embryonic defects. The *Hand2* systemic knock-out results in lethality by embryonic day (E)10.5 due to cardiac malformations of the right ventricle and aortic sac.[26] Conditional ablations of *Hand2* within neural crest cells (NCC) reveal that the gene is required for the neurons in the sympathetic ganglia to express the noradrenergic phenotype that distinguishes the majority of the postganglionic neurons.[26] Loss of *Hand2* in NCC also leads to jaw development defects, including a cleft palate, a hypoplastic mandible and aglossia in mouse embryos.[27–30] Within cardiac NCC, the loss of *Hand2* results in the misalignment of the cardiac outflow tract (OFT) and the aortic arch arteries, allowing for the development of double outlet right ventricle and ventricular septal defects.[23,31] During limb morphogenesis, *Hand2* is expressed in the posterior limb mesenchyme where it shows mutual antagonism with GLI3 and is required for posterior expression of the secreted ligand Sonic hedgehog (*Shh*), likely via direct binding to the zone of polarizing activity regulatory sequence (ZRS).[20,22,32] This interaction establishes an autoregulatory loop with Shh, setting the register for digit identity.[20,33,34] HAND2 also acts antagonistically with TWIST1 during limb development; and in humans, this antagonism plays a role in the autosomal dominant disease Saethre Chotzen Syndrome (SCS).[35,36] Although the necessity of *Hand2* during embryogenesis is well-established, the transcriptional regulation of *Hand2* is less understood. Despite the presence of an extensive (>500 kb) non-protein coding genomic interval flanking *Hand2* on the 5′ and harboring multiple limb enhancers,[37,38] the current view is that cardiac and neural crest *Hand2* expression is predominantly controlled by two separate enhancers located immediately upstream of *Hand2*, with potentially additional cardiac enhancers located in upstream or downstream regulatory regions.[12,13,39] A 208 bp pharyngeal arch (PA) enhancer around 7 kb upstream of *Hand2* is required for *Hand2* expression within the distal and medial post-migratory neural crest that compose mandibular component of PA 1 and 2 in mice.[12] The PA enhancer requires Endothelin-1 activity and it was shown that the Homeobox transcription factor DLX6 (and likely DLX5) can directly bind the four conserved *cis*-elements within this enhancer.[12] A second 1.5 kb GATA-dependent *Hand2* enhancer was discovered to drive *Hand2* expression within the right ventricle (RV) and OFT cardiomyocytes.[11–13,40] This enhancer does not show any expression in the pharyngeal mesoderm of the second heart field where *Hand2* is robustly expressed. Indirect evidence in endocardial cells revealed that HAND2 lies within the NOTCH gene regulatory network[41,42]; however, the transcriptional enhancer that drives *Hand2* expression within the NOTCH network is currently unidentified. Collectively, the enhancers that drive *Hand2* within the endocardium, epicardium, sympathetic and enteric nervous systems, blood, and maternally derived decidua remain unidentified.

In this study, we decided to interrogate the 200 kb genomic upstream region flanking the *Hand2* gene body and including the *Upperhand* (*Uph*) long non-coding RNA (lncRNA) locus[43] for the presence of yet unidentified transcriptional enhancers. Analysis of recently published H3K27ac profiles across multiple mouse embryonic tissues and timepoints[44] revealed two conserved enhancer-like elements in the 200 kb region located 106 kb (−106 kb) and 186 kb (−186 kb) upstream of the *Hand2* Transcriptional Start Site (TSS). Using LacZ transgenic reporter mouse lines, we reveal that both predicted enhancer CNSs drive reporter expression in distinct tissues during embryonic development. The *lacZ* expression pattern driven by the 1.7 kb genomic element containing the CNS located −106 kb upstream of the *Hand2* TSS corresponds to a subregion hallmarked by *Hand2* expression within the developing stomach. Interestingly, the −186 kb element (spanning 1.6 kb) consistently drives transcription within the anterior subectodermal mesenchyme of both the forelimbs and hindlimbs in which neither *Hand2* nor *Uph* lncRNA are expressed. Given this enhancer is active in a transgenic scaffold yet silent within the chromatin context of *Hand2* during limb morphogenesis indicates either a complex regulation relative to *Hand2* expression or an alternative target of the enhancer, potentially within a neighboring TAD.

2 | RESULTS

2.1 | Prediction of two transcriptional enhancer elements in the proximal *Hand2* upstream regulatory interval

Using high-resolution HiC datasets from mouse embryonic stem cells (mESCs)[45] we first visualized the basic

chromatin domain structure at the *Hand2* locus. *Hand2* is flanked by topologically associated chromatin domains (TADs) which suggest largely separated interactions with upstream and downstream regulatory components (Figure 1A). Harnessing H3K27ac datasets generated by ENCODE[44] we carried out an in silico evaluation of open chromatin CNSs in the *Hand2* locus to define putative tissue specific enhancers active in *Hand2* expressing tissues (Figure 1A, B). Interestingly, integrative ENCODE peak calling across examined tissues by general 7-group candidate *Cis*-Regulatory Elements (cCREs) indicated only two putative enhancer elements in the whole 200 kb *Hand2* upstream genomic interval, located 186 kb (−186 kb) and 106 kb (−106 kb) apart from the *Hand2* TSS, respectively (Figure 1A, B). Both elements displayed deep sequence conservation down to *Coelacanth* but H3K27ac enrichment at these elements in embryonic tissues at E11.5 from mouse limb, heart, and facial prominence, tissues known for Hand2 functions, was rather moderate (Figure 1B). However, while the −106 kb element showed a specific H3K27ac peak in stomach tissue at E14.5, the −186 kb module revealed significant H3K27ac enrichment in the heart at later stages (E15.5, E16.5, P0, 8w; Figure 1C), providing a rational for interrogation of this region for transcriptional activity. We therefore generated stable transgenic enhancer reporter mouse lines to assess both the −186 kb and −106 kb elements for their *in vivo* enhancer activity potential during mammalian organogenesis.

2.2 | A distant *Hand2*-upstream enhancer is associated to specific control of *Hand2* in the developing mouse stomach

We first assessed the potential of the CNS located −106 kb upstream of the *Hand2* TSS and placed the 1.7 kb genomic element containing the conserved core in front of a LacZ reporter and a minimal Hsp68 promoter[46] (Figure 2A). Eight out of 15 founders displayed an internal X-gal staining pattern that becomes visible at E11.5 and seven founders exhibited no X-gal staining (Figure 2B). Strikingly, as predicted by the H3K27ac profiles, within the expressing founder lines, X-gal staining of E11.5 and E12.5 sections revealed pronounced LacZ signal within tissues of the developing stomach (s; Figure 2C, D). Beyond these stages, the −106 kb element exhibited DNase hypersensitivity at P0 and H3K27ac enrichment within this CNS from E14.5 through birth (P0) (Figure 2D). Sequence alignment revealed considerable sequence identity between mouse, rat, and human and contained a number of conserved *cis*-elements including E-boxes (binding bHLH factors such as HAND2) as well as SOX10, GATA, and Phox2b motifs (Figure 3). Sox10 is an early specifier of neural crest, which contributes to the peripheral nervous system such as the enteric neurons as well as glia.[47] GATA4 and GATA6 factors are known to regulate both *Hand1* and *Hand2* within the pharyngeal arches.[11–13] PHOX2b has been described as an upstream regulator of *Hand2* within neural crest and plays an important role in enteric neurogenesis.[21,41,48]

To determine if this isolated CNS exhibiting stomach enhancer activity represents a subdomain of the *Hand2* mRNA expression pattern, we carried out in situ hybridization (ISH) on E13.5 stomach sections using a *Hand2* probe. This revealed that *Hand2* is expressed within the outer wall of the stomach (s; Figure 4A). Given HAND2 is known to play an important role in the enteric nervous system[49–51] and sympathetic ganglia,[52] we interrogated expression of *Phox2b*, an upstream regulator of *Hand2* in SNS precursors,[53] to mark neuronal tissues in a serial section (Figure 4B). Results showed that neuronal expression of *Phox2b* is more restricted but overlaps with the *Hand2* expression pattern (Figure 4A, B). HAND2 is also known to be expressed within smooth muscle of the OFT.[54] To delineate *Hand2* expression within smooth muscle, we analyzed *Sm22* expression (Figure 4C).[55] Our results show that *Sm22* expression appears internally within the stomach layers; however, there is still overlap with the *Hand2* expression domain suggesting *Hand2* is expressed in both neuronal and smooth muscle cell lineages.

To define the −106 kb stomach enhancer activity in more detail, we analyzed LacZ reporter activity in stomach sections at E13.5 (Figure 4D). In wholemount view, the majority of X-gal staining was observed within the antrum (a) with little to no observable staining within the esophagus (es) or forestomach (fs; Figure 4D). The most caudal section showed detectable staining within the outer mesenchyme (mes) but absent from the medial mesenchyme and epithelium (sp; Figure 4D, i and ii). Progression towards the esophagus showed more robust X-gal staining within the mesenchyme of the outer wall and medial mesenchyme expression becomes visible. The most rostral sections revealed LacZ reporter activity in all the visible stomach mesenchyme as well as the epithelium (Figure 4D, iii and iv). The esophagus exhibited no significant X-gal staining.

We next sought to confirm the activity profile of this enhancer within both smooth muscle and enteric neurons using immunohistochemistry (Figure 5). Using antibodies specific for β-Galactosidase (B-GAL) and α-smooth muscle actin (α-SMA) to define enhancer activity in E13.5 stomach sections demonstrated significant overlap of −106 kb-LacZ reporter activity and α smooth muscle actin expression (Figure 5A–H), revealing that this novel *Hand2* enhancer is expressed within the visceral smooth muscle of the stomach. We next explored

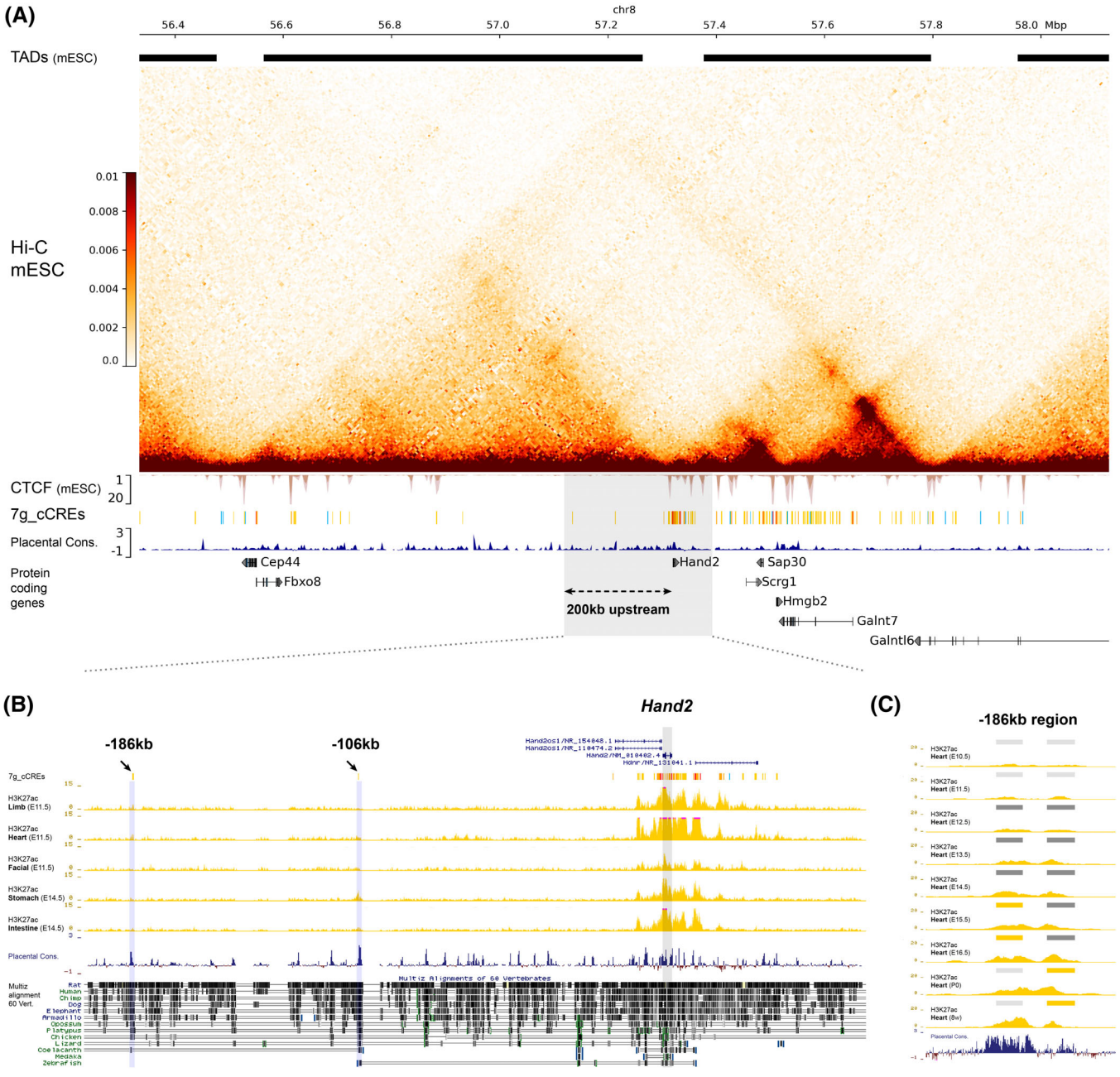

FIGURE 1 (A) Hi-C interaction heatmap, TAD calls and CTCF profiles from ES cells[45] illustrating the chromatin domain structure across the extended *Hand2* locus (mm10, chr8:56334398–58126455). The general 7-group cCRE track from ENCODE (https://screen.encodeproject.org) highlights predicted promoter-like elements (red), enhancer-like sequences (ELS, yellow), CTCF-only sequences (blue) and DNase-only sequences (green).[44] The track below shows the vertebrate conservation profile (phyloP60way). Protein coding genes in the region are listed and double arrow demarcates the 200 kb interval upstream of the *Hand2* transcriptional start site (TSS). (B) UCSC browser window showing enhancer-predictive H3K27ac signatures at the *Hand2* locus from E11.5 limb, heart, facial tissues as well as E14.5 stomach and intestine as obtained by ENCODE.[44] Peak calls (arrows) represent regions with significant enhancer-predictive H3K27ac (ELS) in any of the tissues examined (ENCODE, general seven group cCREs).[44] The −186 and −106 elements are the only ELS within the 200 kb upstream interval. The proximal peak, located at −106 kb from the *Hand2* TSS, (EM10E0878143, mm10 chr8:57213987–57214326) and distal peak located −186 kb from the *Hand2* TSS (EM10E0878141, mm10 chr8:57134745–57135094) were isolated and tested for enhancer activity in this study. The blue track shows sequence conservation among placentals. The Multiz alignment (in black) shows conservation of sequence identity throughout 60 vertebrate species. (C) UCSC browser screenshot showing H3K27ac profiles at the −186 kb element in mouse hearts between E10.5 and P0 and adult male mice of 8 weeks (8w). Yellow bars indicate enhancer-like sequence by significant enrichment of H3K27ac over background.[44] Gray shades indicate lower H3K27ac enrichment. Lower blue track marks placental conservation indicating the H3K27ac peaks correlate with the higher levels of shared sequence identity.

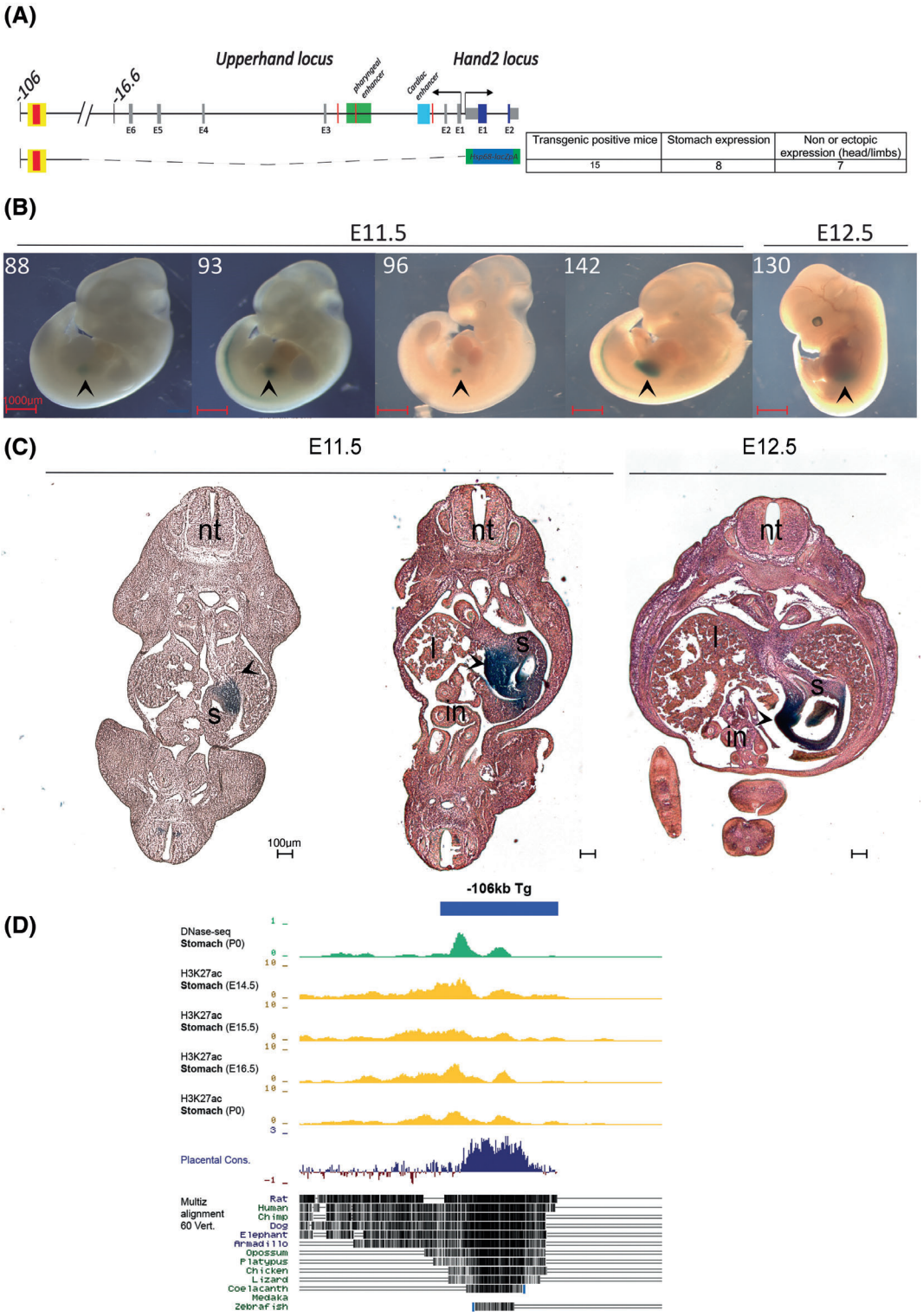

FIGURE 2 Identification of a *Hand2* stomach enhancer. (A) 1.7 kb of genomic sequence containing the CNS located 106 kb upstream (−106b) of *Hand2* and *Uph* TSSs (arrows) was cloned in front of an *Hsp68* minimal promoter and *LacZ* reporter construct for production of transgenic mouse lines. *Hand2* non-coding (gray) and coding sequence (blue) are demarcated. *Uph* exons are marked gray and conserved non-coding sequence is depicted in red (within the yellow box). Green and blue boxes indicate the location of the pharyngeal arch[11] and right ventricle[13] enhancers, respectively. $N = 15$ transgenic mouse lines were assayed with embryos from $n = 8/15$ lines showing consistent stomach expression between E11.5 and E12.5. Embryos from $n = 7/15$ mouse lines exhibited no or inconsistent expression within the head or limbs. (B) Five independent lines showing stomach specific expression (arrowheads). Line 142 was used for the remainder of this study. Scale bars, 1 mm. (C) Transverse sections through E11.5 and E12.5 showing expression is within the stomach (s, arrowheads). No β-galactosidases expression is observed within the intestine (in), liver (l), or neural tube (nt). Scale bars, 100 µm. (D) DNase hypersensitivity (green track) at the *Hand2* −106 kb CNS element revealing open chromatin at P0 and strong H3K27ac enrichment (yellow tracks) ranging from E14.5 through P0. Placental conservation and sequence alignment of specific vertebrates are shown.

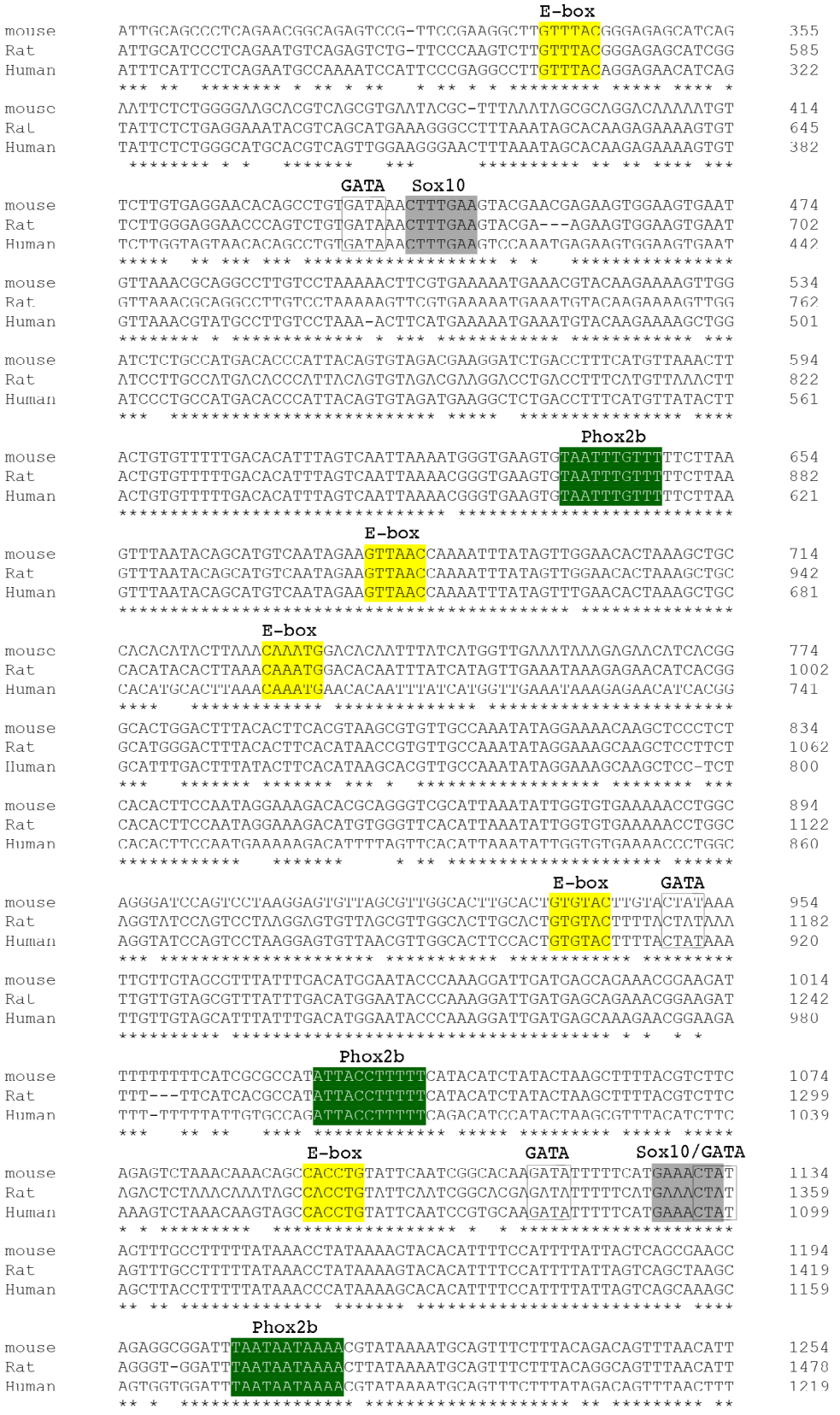

FIGURE 3 Evolutionary conservation reveals a number of putative *cis*-elements that could be at play regulating enhancer activity. Analysis of mouse, rat, and human sequence within the core region of the *Hand2* −106 kb stomach enhancer reveals the presence of $n = 3$ GATA (open boxes), $n = 2$ SOX10 (gray), $n = 3$ PHOX2b (green), and $n = 5$ E-box (yellow) consensus sequences.

β-Galactosidase co-expression with the pan-neuronal marker Tubulin β3 (TUBB3; Figure 5I–P) illustrating that TUBB3 + cells occupy a narrow band of cells near the luminal edge and that these cells are also positive for β-Galactosidase (Figure 5I–L). Additionally in regions with significant smooth muscle, TUBB3+ neurons were also positive for β-Galactosidase (Figure 5M–P, see expression overlay).

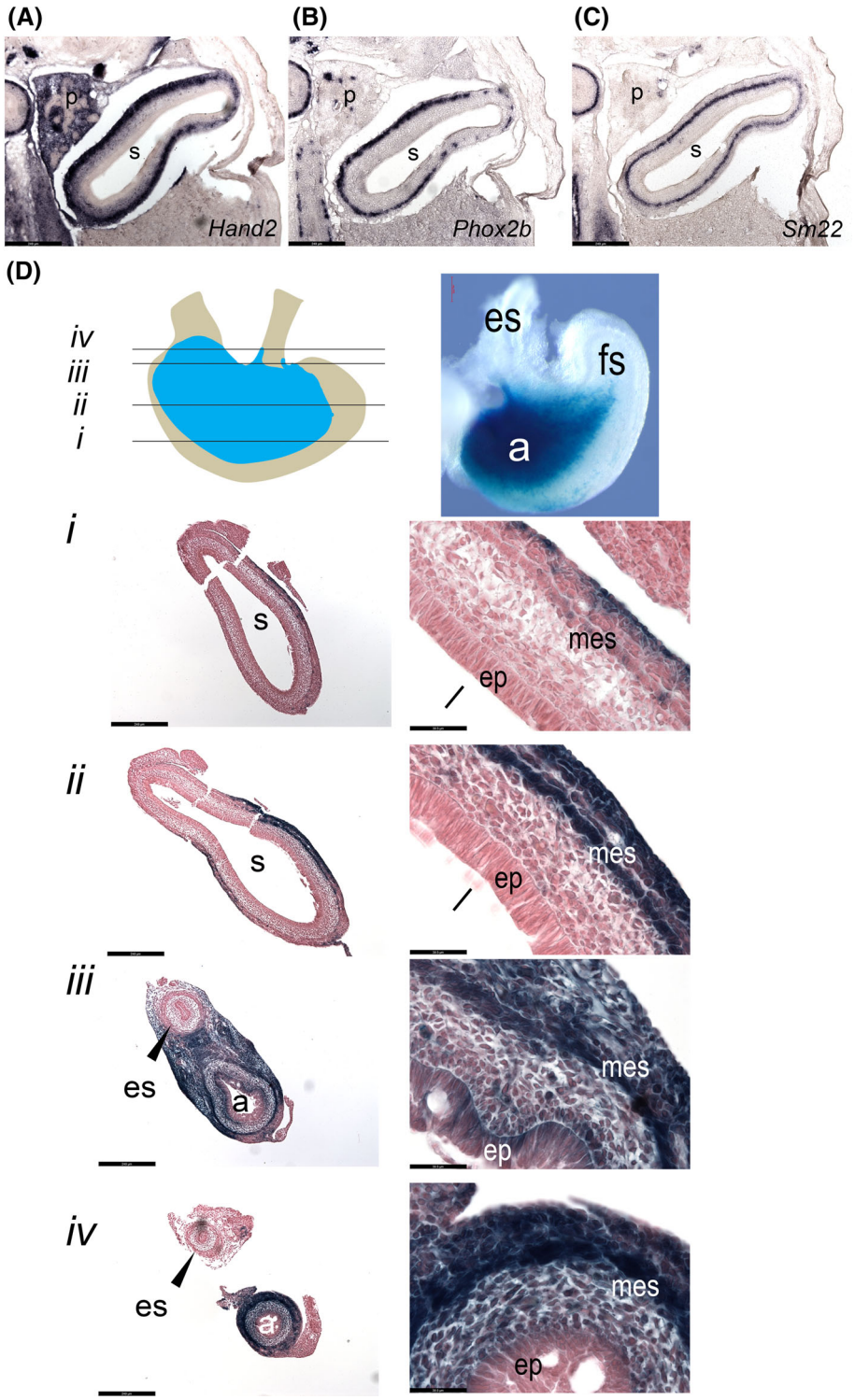

FIGURE 4 *Hand2* expression in the developing stomach at E13.5. (A) ISH of *Hand2* showing expression within the outer wall of the stomach (s) and pancreas (p). (B) ISH of *Phox2b* marking the developing enteric nervous system within a serial section. (C) ISH of *Sm22* marking the developing smooth muscle within a serial section. Scale bar, 250 μm. (D) Whole-mount and section expression analysis of the *Hand2* stomach enhancer (−106 kb-*Hsp68*-LacZ reporter) at E13.5. Illustration of the whole-mount expression plane of section is denoted by lines and isolated stomach showing robust expression within antrum (a) and low or undetectable expression within the forestomach (fs). *i* and *i′* show a caudal section through the stomach (s) were β-galactosidase staining is observed within the outer wall mesenchyme (mes) but not within the epithelium (ep) at the luminal surface-stained stomach. Scale bar, 200 μm. (l) *ii*) and *ii′*) show a more rostral section where robust staining in the outer layers of the stomach is observed. *iii* and *iii′*) show a further rostral section exhibiting deeper β-galactosidase staining that approaches the epithelium but does not surround the esophagus (es). *iv* and *iv′* at the level of the upper antrum and esophagus reveal broad staining around the stomach entrance that is largely excluded from around the esophagus. Lower magnification images *i–iv*. Scale bar, 250 μm. High magnification images *i–iv*. Scale bar 39.5 μm.

2.3 | The CNS located 186 kb upstream of *Hand2* drives expression in the murine *Hand2*-negative distal-anterior limb mesenchyme

The second and more distal enhancer-like CNS defined within the interrogated 200 kb *Hand2* upstream interval lies 186 kb upstream of the *Hand2* TSS (Figure 1A, B, C). Using our LacZ reporter framework, we assessed the regulatory activity of this element (spanning 1.6 kb) during embryogenesis by generating stable transgenic mouse lines (Figure 6A), analogous to the analysis of the −106 kb stomach enhancer. Eleven transgenic founders were obtained and tested for enhancer activity at E11.5 (Figure 6B, C). Surprisingly, despite the absence of significant H3K27ac peaks in limbs between E10.5 and E15.5

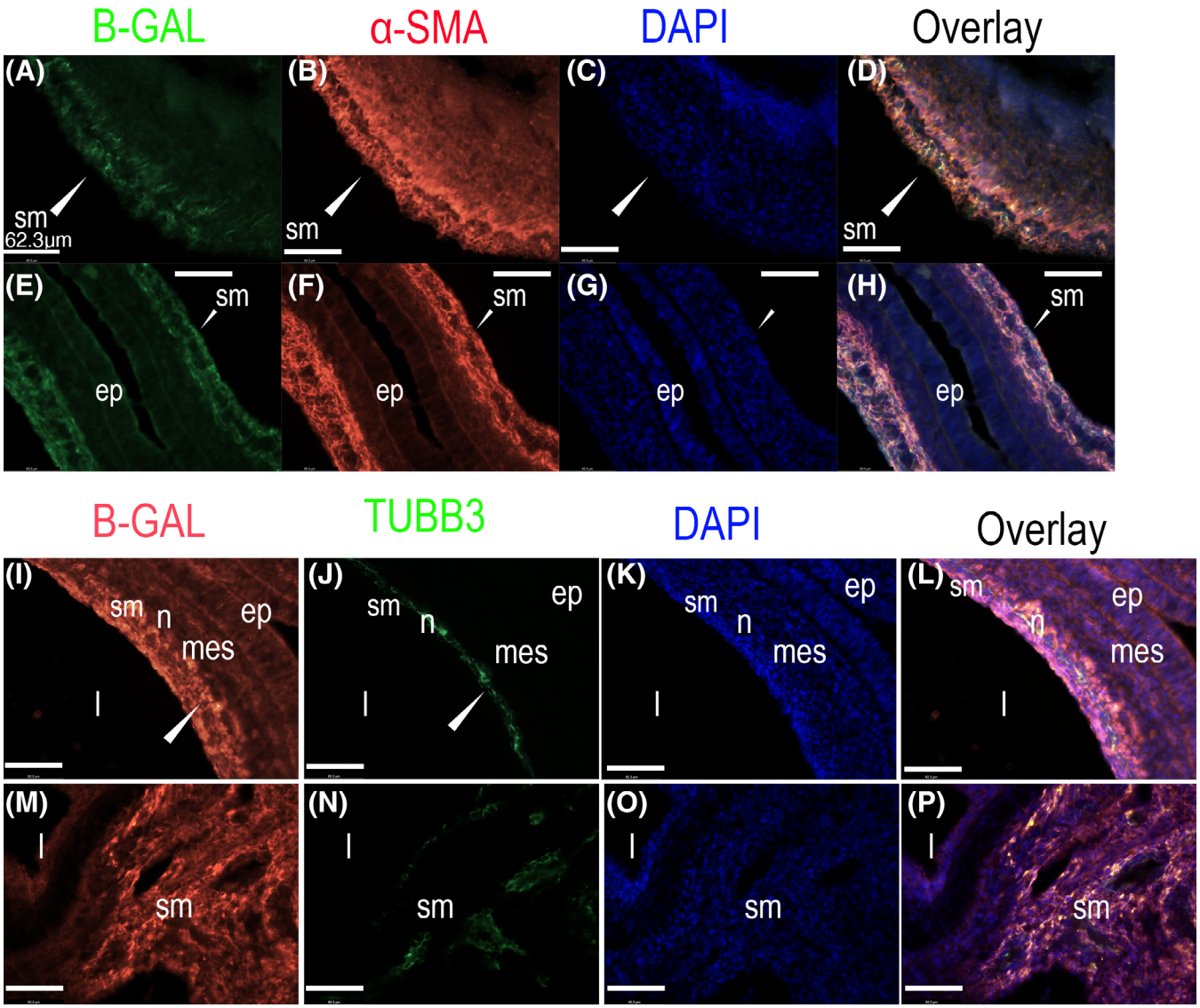

FIGURE 5 *Hand2* stomach enhancer expression largely overlaps with smooth muscle and neurons. (A–H) E13.5 mouse embryonic sections that were immunostained for β-Galactosidase (B-GAL) and smooth muscle (sm) alpha actin (α-SMA), along with a nuclear DAPI counterstain. Four section planes (A, E, I, and M) through the stomach reveal near complete overlap with α-SMA (red) and B-GAL (green). Similarly, E13.5 stomach sections were immunodetected for B-GAL (red) and the neuron (*n*) specific TUBB3 protein (green). Although B-GAL reactivity is broader than TUBB3 signal (potentially reflecting different sensitivities) it indicates reporter localization to enteric neurons. ep, epithelium; l, lumen; mes, mesenchyme. Scale bars, 62.3 μm.

of development (Figure 6D), our transgenic results demonstrated CNS driven reporter activity specifically within dorsal and ventral surfaces of the anterior limb bud in five of the 11 founder lines (Figure 6C), while the remaining lines did not display any β-galactosidase activity. In addition, DNase-seq accessible chromatin profiling from ENCODE revealed the presence of a protein complex at the conserved core of the −186 kb element, indicating potential involvement of a mechanism that suppresses anterior limb enhancer activity under endogenous conditions (Figure 6D).

Sequence conservation of the −186 kb element throughout mammals and canary is significant with a number of *cis*-elements including MEF2, TBX2, 3, and 5 motifs that exhibit complete or near complete conservation among species (Figure 7). MEF2 transcription factors play critical roles in defining numerous tissues including smooth, and skeletal muscle.[56] T-box transcription factors are well established in limb development[57] and *Tbx3* has an established genetic interplay with *Hand2*.[58] Moreover, TBX5 mutations are causative of Holt Oram syndrome affecting forelimbs and heart.[59]

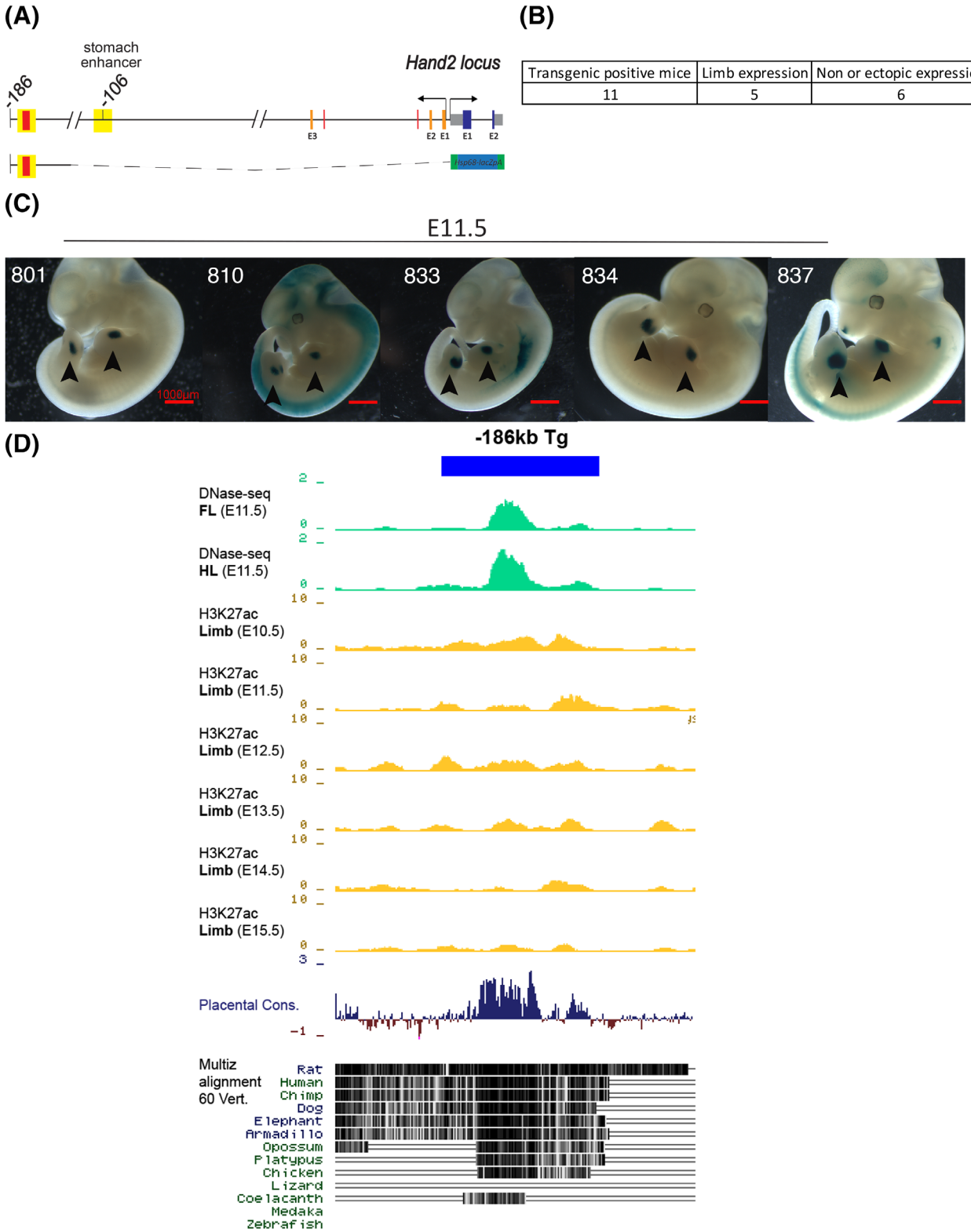

FIGURE 6 The *Hand2* −186 kb element displays anterior limb enhancer activity. (A) 1.6 kb of conserved non-coding sequence (mm10, chr8:57133607–57135181) located 186 kb upstream to the *Hand2* and *Uph* TSSs (arrows) was cloned and inserted upstream of a *Hsp68-LacZ* transgenic reporter cassette. *Hand2* non-coding (gray) and coding sequence (blue) are denoted. *Uph* exons (only up to exon 3) are denoted in orange and conserved non-coding sequence shown in red within the yellow box. (B) Embryos from 11 transgenic mouse lines were assayed and $n = 4/11$ were showing consistent limb expression starting at E11.5. Embryos from $n = 6$ mouse lines exhibited no or inconsistent expression. Scale bars, 1000 µm. (C) All five independent lines showing limb specific expression (arrowheads) are shown. Line 801 was used for the remainder of this study. (D) DNase hypersensitivity from fore- and hindlimbs (FL, HL: green tracks) at E11.5 along with H3K27ac profiles across multiple stages (yellow tracks) from ENCODE (SCREEN). The blue bar demarcates the 1.6 kb sequence interval selected for reporter transgenesis in this study. Placental conservation track is shown below.

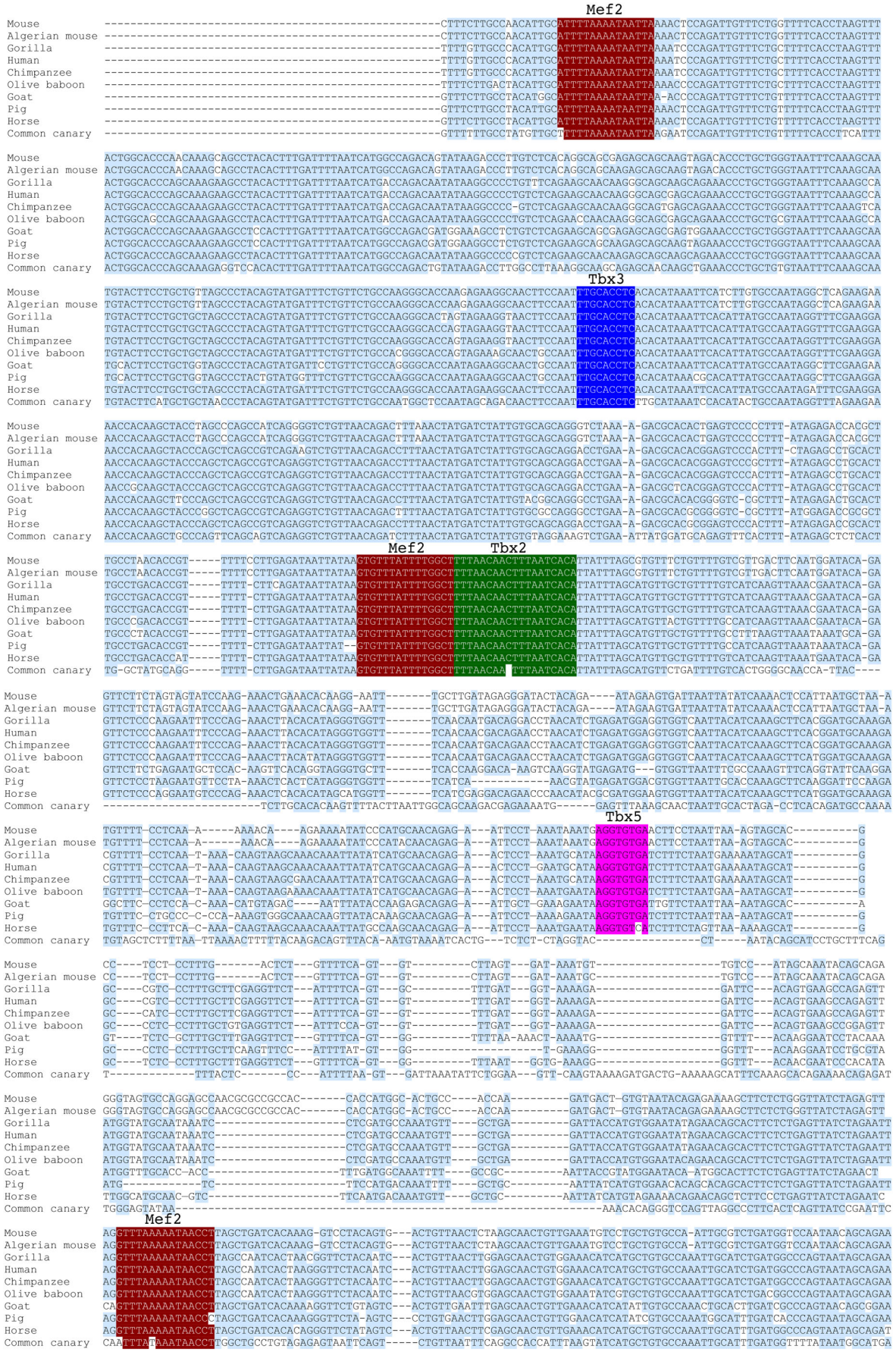

FIGURE 7 Legend on next page.

Given that the reproducible activity of the −186 kb element does not appear to overlap *Hand2* expression in early developing limbs,[20,22,36] we compared −186 kb reporter activity with *Hand2* and *Uph* expression in limbs at E11.5 using ISH (Figure 8). Results from wholemount embryos corroborate that *Hand2* and *Uph* are predominantly expressed within the posterior (p) fore- and hindlimb (fl and hl) mesenchyme including the zone of polarizing activity (ZPA; Figure 8A, B, D, E). This contrasts with the activity of the −186 kb CNS localized strictly within the anterior (a) domain of E11.5 fore- and hindlimbs (Figure 8C, F). These observations were confirmed by section ISH and X-gal staining of E11.5 embryos, respectively (Figure 8G–L), demonstrating that both *Hand2* and *Uph* mRNA are detectable in posterior fore- and hind-limbs and show expression that reaches the dorsal most portion of the limb buds (Figure 8G, H, J, K). X-gal stained sections containing more anterior regions of the limb buds from embryos encoding the −186 kb LacZ reporter transgene revealed that the enhancer activity is localizing to the dorsal and ventral subectodermal limb mesenchyme but does not reach the limb midline at the apical ectodermal ridge (Figure 8I, L). Analysis of *Hand2*/*Uph* expression and −186 kb activity patterns in hindlimb sections further corroborated the lack of pattern overlap (Figure 8J, K).

Although the Hi-C data from mESCs indicate minor chromatin contacts between *Hand2* and the nearest cluster of downstream genes (Figure 1), correlation of published expression data from E10.5 and E11.5 limbs for the 3′ genes *Sap30* and *Hmgb2* identified from the EMAGE and MGI databases[60–64] indicates partial overlap of −186 kb element activity with the anterior expression domain of these genes (Figure 9A). To investigate potentially differential chromatin interactions in the developing limb, we mapped interaction counts from Hi-C data of distal limb mesenchyme at the *Hand2* locus and neighboring TADs[65] (Figure 9B). Analysis of these limb Hi-C interactions in comparison to CTCF DNA occupancy data from mouse ES cells[45] indicated only minor contacts of the −186 kb element with *Sap30* or *Hmgb2* (blue arrowheads, Figure 9B), similar to the domain structure and interactions in mESCs (Figure 1A). In contrast, contacts with *Hand2* appeared stronger in both datasets, suggesting that the −186 kb element is more frequently contacting *Hand2* in distal limbs.

3 | DISCUSSION

In this study, we identified two novel transcriptional enhancer sequences within the *Hand2* locus. The first, located −106 kb upstream of the *Hand2* TSS, drives specific expression within the antrum of the stomach within smooth muscle and potentially enteric neural crest derived neurons (Figures 2, 4, and 5). The stomach is derived from the posterior foregut along with the esophagus, liver, gallbladder, pancreas and intestine.[66,67] Hedgehog signaling and the transcription factor GATA4 play important roles in stomach smooth muscle formation.[66,67] Interestingly, both GATA and SHH are established as regulators of *Hand2* expression within the heart, and pharyngeal arches, limbs, and enteric neurons.[12,13,22,49,50,68] Conserved binding motifs are present within the −106 kb sequence for GATA (open boxes), the enteric neuron expressed SOX10 (gray boxes) and PHOX2b (green boxes) (Figure 3). *Hand2* is expressed within post migratory neural crest cells as well as the lateral plate mesoderm within the early embryo[26,69,70] and its continued expression within organ smooth muscle and autonomic neurons is expected. The robust -106kb-LacZ reporter activity observed in the mesenchymal layers of the developing stomach (Figure 4) supports this notion. Moreover, immunofluorescence data shows significant overlap of β-galactosidase expression and that of smooth muscle α Actin and Tubulin β2 (Figure 5) within the restricted antrum domain of the enhancer. What makes this observation most interesting is that this region is responsible for mucus and gastrin secretion and exhibits an absence of WNT signaling that is robust in more rostral structures where *Hand2* expression appears excluded.[67] Given that the entire stomach is innervated and sheathed in a smooth muscle layer, it is intriguing that this *Hand2* stomach enhancer is active outside of the established WNT signaling domain. We conclude that this stomach enhancer is likely controlling *Hand2* expression; however, without using gene editing to remove the sequence and interrogate *Hand2* stomach expression, we cannot rule out participation of additional stomach enhancers in other *Hand2* *cis*-regulatory regions, for example as part of partially redundant enhancer systems.[8]

The most surprising of our findings was that the element located 186 kb upstream to the *Hand2* TSS (−186 kb) drove activity in the *Hand2*-non overlapping distal-anterior limb mesenchyme. Five of the 11 lines

FIGURE 7 Evolutionary conservation of the *Hand2* −186 kb limb enhancer element. The sequence core is well conserved throughout mammals and canary. The identification of conserved motifs for MEF2 (maroon shade), TBX3 (blue shade), TBX2 (green shade), and TBX5 (pink shade) indicate transcriptional enhancer identity of this sequence.

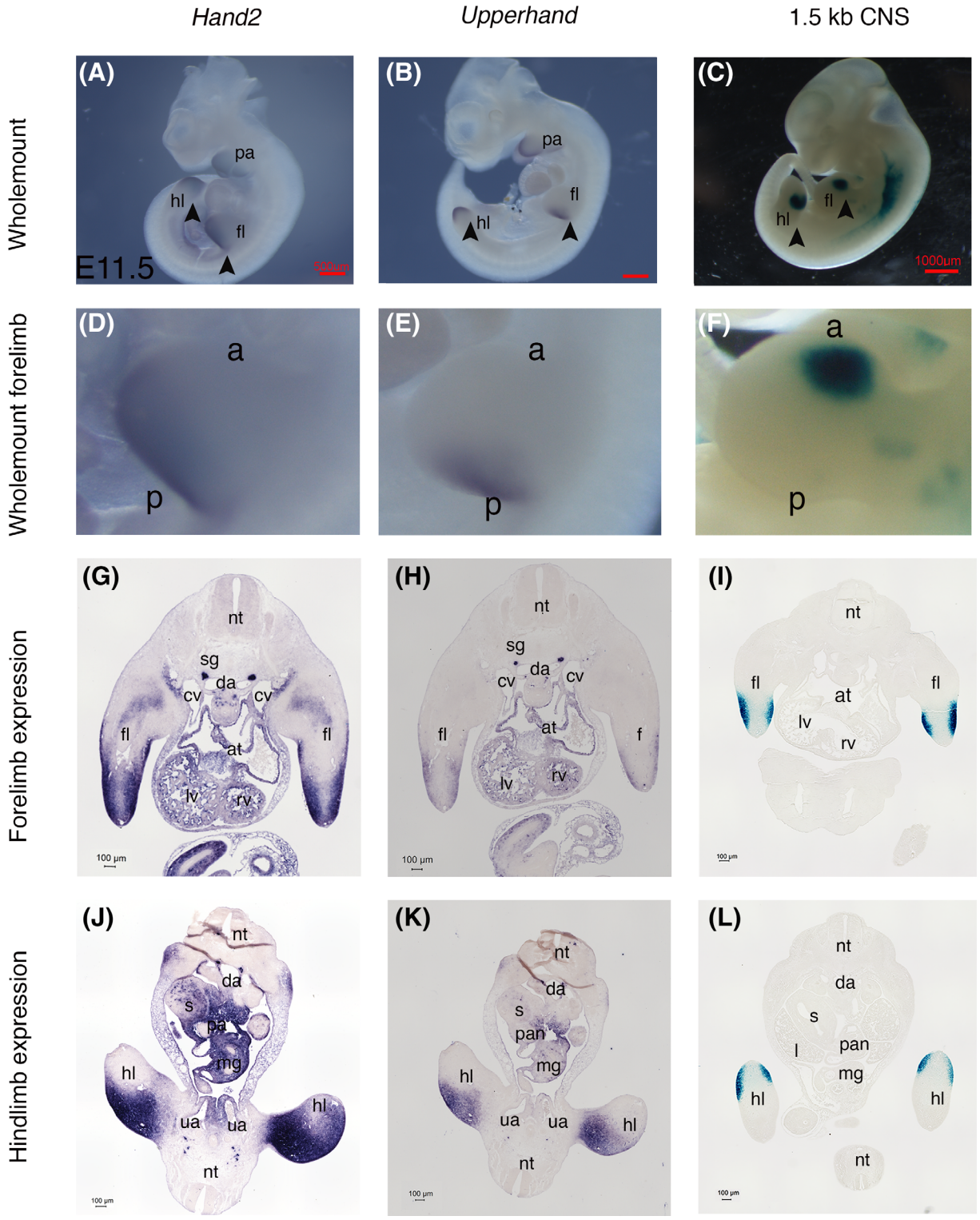

FIGURE 8 Expression of the *Hand2* −186 kb limb CNS does not overlap with *Hand2* or *Uph* expression. (A) Whole-mount ISH at E11.5 showing *Hand2* expression within the pharyngeal arches (pa), fore- (fl) and hindlimbs (hl) and heart. (B) Whole-mount ISH at E11.5 revealing the *Uph* expression pattern which is similar to *Hand2*. (C) β-galactosidase staining in the anterior portion of the limb in −186 kb-*Hsp68*-LacZ reporter embryos for comparison with *Hand2* and *Uph* expression indicates mutually exclusive patterns. (D–F) Close-up images of the forelimbs shown in A–C. (G–L) Section ISH and section β-galactosidase staining showing the lack of pattern overlap between *Hand2* and *Uph* mRNA and −186 kb enhancer activity. a, anterior; p, posterior; nt, neural tube; at, atria; rv, right ventricle; lv, left ventricle; da, dorsal aorta; cv, cardinal vein; sg, sympathetic ganglia; s, stomach; l, liver; pan, pancreas; mg, midgut ua, umbilical artery. Red scale bars for whole-mount embryos, 500 or 1000 µm. Scale bars for sections, 100 µm.

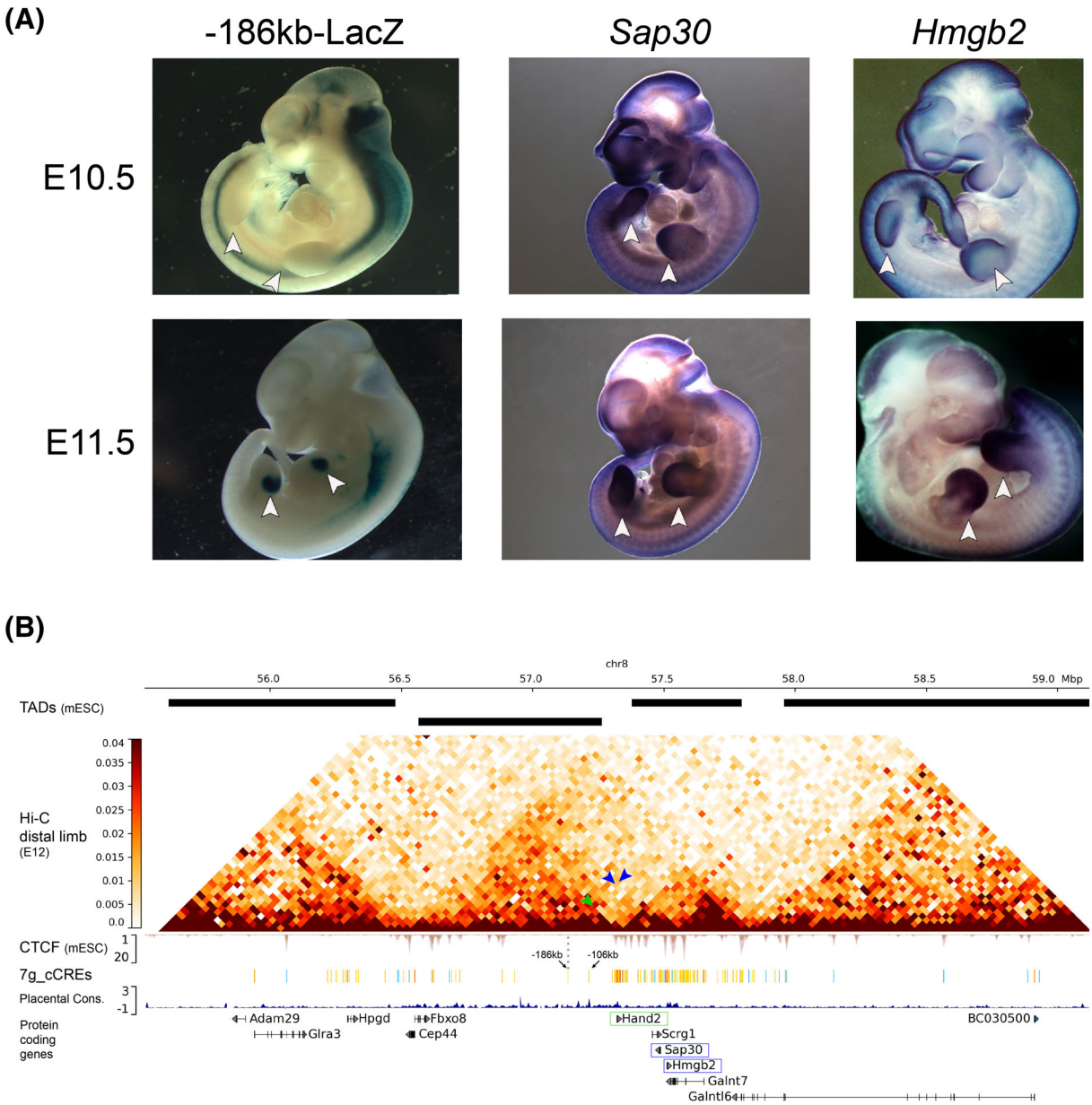

FIGURE 9 (A) Comparison of the anterior limb enhancer activity of the *Hand2* −186 kb CNS with the limb expression domains of the *Sap30* and *Hmgb2* genes in mouse embryos. *Sap30* whole mount ISH obtained from the Jaxson lab MGI database (E10.5 https://www.informatics.jax.org/image/MGI:5820626; E11.5 https://www.informatics.jax.org/image/MGI:5820631 with permission from Steven Vokes).[60,61] *Hmgb2* data for E10.5 was obtained from the mouse atlas EMAGE (https://www.emouseatlas.org/gxdb/dbImage/segment1/2859/detail_2859.html with permission from Andrew McMahon).[62,63] E11.5 was obtained from the mouse atlas EMAGE (https://www.emouseatlas.org/gxdb/dbImage/segment6/28272/detail_28272.html with permission from Hiroshi Asahara) originally deposited at EMBRYS (https://www.embrys.jp/embrys/html/MainMenu.html).[63,64] E, embryonic day. White arrowheads point to embryonic limbs.
(B) Reprocessed Hi–C interaction counts in the distal limb mesenchyme[65] indicate chromatin contacts at the *Hand2* locus and flanking TADs (mm10, chr8:55521203–59121203). TAD calls (Hi–C) and CTCF profiles (ChIP-seq) from mouse embryonic stem cells (mESCs)[45] are shown. General 7-group cCREs from ENCODE (https://screen.encodeproject.org) are listed to indicate promoter-like elements (red), enhancer-like sequences (ELS, yellow), CTCF-only sequences (blue) and DNase-only sequences (green). Vertebrate conservation (phyloP60way) is shown in blue. Heatmap values for −186 enhancer interaction with *Hand2* (green arrow) and limb-expressed *Sap30* and *Hmgb2* genes (blue arrows) are indicated.

generated exhibit reproducible expression within the anterior dorsal and ventral surfaces of the developing limb (Figures 6 and 8). The puzzle is that these domains do not correspond to where *Hand2* or the lncRNA *Uph* are expressed within the forming limb (Figure 8). There are a number of possible reasons for this observation.

Perhaps the simplest possibility is that this enhancer regulates another gene. *Sap30* and *Hmgb2* are the closest genes to *Hand2* showing limb expression patterns overlapping the anterior limb activity domain of the −106 kb element (Figure 9). Physical interaction between the −106 kb element with these genes however appears more unlikely when considering TAD structure at the *Hand2* locus in both mESCs or distal limbs, indicating that the upstream and downstream regulatory interactions of *Hand2* occur in largely partitioned domains (Figure 9).

It is also possible that this CNS is a dormant enhancer in the mouse. Possible mechanisms for this lack of transcriptional activity include chromatin remodeling, which could result in limiting access of the enhancer to transcription factor binding.[71,72] In the context of a transgenic insertion, the enhancer activity would be unmasked from its endogenous chromatin context, similar to recent observations of elements with hidden enhancer characteristics near developmental genes.[73] Given that limb development is one of the most dynamic developmental processes throughout vertebrates, resulting in a wide spectrum of phenotypic outcomes, it is surprising that the transcriptional networks that drive limb morphogenesis in vertebrates are highly conserved. Previous research shows that even minor mutations within highly conserved enhancers can cause significant phenotypic differences.[71,74,75] In enhancer replacement studies where the mouse *Prx1* limb enhancer was substituted with the corresponding CNS enhancer sequences from bat, a significant increase in forelimb length within the mutant mice was observed, demonstrating enhancer evolution among species.[76] Although various mammalian limb enhancers are highly conserved in the snake genome, research has established that the loss of limbs throughout snake evolution is associated with nucleotide mutations in the ZRS, a long-distance enhancer required for posterior *Shh* limb bud expression and normal limb development.[77,78] When snake ZRS enhancers were knocked-in to replace the endogenous ZRS in mice, normal limb development was hobbled.[77,78] Sequence comparisons identified a 17 bp deletion of a ETS1 motif in the snake ZRS as compared with the ZRS of limbed lizards. When the 17 bp sequence was reintroduced into the python ZRS and used to replace the endogenous mouse enhancer, normal limb development was observed in the resultant mice.[77,78] Indeed, some conserved limb enhancers occur in snakes but are not required for limb development suggesting that they may have been retained for gene regulatory networks of other developmental processes. For example, when the *Tbx4* enhancer HLEB is deleted from mice, it presents with defects in the hindlimbs and genitalia. Further analyses in snakes defines the loss of activity of HLEB in the hindlimbs but enhancer activity in the phallus.[79] It has also been shown that enhancers exhibiting high sequence identity can have different functions, and can be expressed and play essential roles in different tissues among species. For instance, vertebrate-conserved *Shh* enhancers drive different neuronal expression patterns in zebrafish and mice, suggesting the enhancer has diverged during evolution between the vertebrates.[80] If indeed the −186 kb enhancer regulates *Hand2*, the observation that an element with limb transcriptional enhancer activity remains silent endogenously in mouse embryos could reflect that it is active in other species potentially contributing to a divergent limb phenotype. However, if the 186 kb enhancer is regulating an unknown gene within a neighboring TAD, likely beyond the one harboring *Sap30* and *Hmgb2* genes, this could suggest a novel chromatin context not yet associated with permissive transcription.

4 | EXPERIMENTAL PROCEDURES

4.1 | Cloning

To generate the −106 kb *Hand2* CNS *Hand2*^{stomach} transgene, the genomic sequence including ENCODE element EM10E0878143 (mm10 chr8:57213987–57214326) was amplified with the forward primer Peak −106 kb (F) 5′-GCTACTCGA*GGCGGAGGAAAGTAGCAGCAT*-3′ and reverse primer Peak −106 kb (R) 5′-GCTAGTCGA*CCGAGCAGAAGGGGCTAGTTC*-3′. The sequence was then cloned into the XhoI site within the multiple cloning sites (MCS) sequence of the *Hsp68-lacZ* reporter construct.[46] The −186 kb CNS including EM10E0878141 (mm10 chr8:57134745–57135094) was amplified using forward primer Peak −186 kb (F): 5′-GTCACTCGA*GTAGAAGTGGCAATGTCTAAG*-3′ and reverse primer Peak −186 kb (R) 5′ GTCACTGCA*GCTAGTATTTACTCTTTAGGG*-3′. The sequence was then cloned into the XhoI site within the multiple cloning sites (MCS) sequence of the same *Hsp68-lacZ* reporter construct.

4.2 | Experimental mice

The University of Michigan Transgenic Animal Model Core generated the founders of both the −106 and −186 kb transgenic mouse lines on a C57BL/6 and SJL mixed background. Genotyping of the -106kb-LacZ mice was performed either via Southern blot using a 311 bp *LacZ*-specific probe as described[81] or PCR using the forward primer *Hand2*-106 kb 1.7 CNS(F) 5′-CTACAA GAACAAATGGCGGTGA-3′ and the reverse primer

Hsp68(R) 5′-GCCTCTGACCTCATGGACTAATTT-3′, which produces a 592 bp amplicon that detects the presence of the transgene. After a 2 min incubation at 94°C, the PCR run conditions are 94°C 60 s, 60°C 30 s, and 72°C 30 s for 32 cycles. Genotyping of the -186kb-LacZ mice was performed via PCR using the forward primer H2-186kb 5′ CCTAATTAAAGTAGCACGCCTCC-3′ and Hsp68(R) using the aforementioned PCR conditions.

All animal maintenance and procedures were performed in accordance with the Indiana University School of Medicine protocol 20090, and University of Michigan School of Medicine.

4.3 | X-gal staining and histology

X-gal staining and histological preparations were performed as previously described for paraffin sections, cryosections, and wholemounts.[21,41,48]

4.4 | In-situ Hybridization

Section ISH was performed on 10–12 μm paraffin sections as previously described.[10,82] Wholemount ISH was carried out on whole embryos as described.[83] Antisense digoxygenin-labeled riboprobes were synthesized using T7, T3, or SP6 polymerases (Promega) and DIG-Labeling Mix (Roche, Basel, Switzerland) using plasmid templates for: *Hand2*,[84] uppderhand,[43] *Phox2b*,[48] and *Sm22*.[55,85]

4.5 | Reprocessing of HiC-data

The mESC Hi-C map of the extended *Hand2* TAD was generated by filtering (MAPQ30) available valid read pairs re-analyzed using HiCUP v.0.6.1 (GSE161259), originally derived from Bonev et al. (GSE96107).[45] The reanalysis procedure and code used to generate the representation of the HiC map is available on https://github.com/lldelisle/Hi-C_reanalysis_Bonev_2017.[45] The *Hand2* chromatin contact map from wildtype (WT) distal mouse embryonic limbs (DL) at E12.0 was generated using a published Hi-C dataset (GSE101715).[65] Briefly, raw.cool format Hi-C maps were generated through the "cooler cload tabix" tool (Cooler v0.8.11), loading native chromosome 8 genomic interval (mm10, chr8:55400000–59200000 for mESC, chr8:55521203–59121203 for DL) validated pairs[65] into a matrix of fixed bins (5 kb resolution for mESC, 30 kb for DL). For further normalization and diagonal filtering, the Cooler matrix balancing tool[86] was applied with the options "–mad-max 5 –min-nnz 10 –min-count 0 –ignore-diags 2 –tol 1e-05 –max-iters 200 –cis-only", resulting in balanced "cool" maps as final output. The matrix heatmaps were plotted using pygenometracks.[87]

ACKNOWLEDGMENTS

Infrastructural support at the Herman B Wells Center for Pediatric Research is in part supported by the generosity of the Riley Children's Foundation, Division of Pediatric Cardiology, and the Carrolton Buehl McCulloch Chair of Pediatrics. This study is supported by the NIH grants 1R01DE02909; 1R01HL145060; 2P01HL134599; and 1R01HL120920 to Anthony B. Firulli and a Swiss National Science Foundation (SNSF) grant PCEFP3_186993 to Marco Osterwalder. We thank Danny Carney for excellent technical assistance. We also thank the Olson Lab for providing the *Uph* riboprobe.

CONFLICT OF INTEREST STATEMENT

The authors declare no potential conflicts of interest.

DATA AVAILABILITY STATEMENT

We agree to make all mice engineered by us and all data freely available.

ORCID

Marco Osterwalder https://orcid.org/0000-0002-1969-2313

Anthony B. Firulli https://orcid.org/0000-0001-6687-8949

REFERENCES

1. Tyser RCV, Mahammadov E, Nakanoh S, Vallier L, Scialdone A, Srinivas S. Single-cell transcriptomic characterization of a gastrulating human embryo. *Nature*. 2021;600(7888):285-289. doi:10.1038/s41586-021-04158-y
2. Rossant J, Tam PPL. Early human embryonic development: blastocyst formation to gastrulation. *Dev Cell*. 2022;57(2):152-165. doi:10.1016/j.devcel.2021.12.022
3. Bruneau BG. The developing heart: from the wizard of Oz to congenital heart disease. *Development*. 2020;147(21):1-6 doi:10.1242/dev.194233
4. Gonzalez-Teran B, Pittman M, Felix F, et al. Transcription factor protein interactomes reveal genetic determinants in heart disease. *Cell*. 2022;185:794-814. doi:10.1016/j.cell.2022.01.021
5. Gunsagar S, Gulati SSS, Wesche DJ, et al. Single-cell transcriptional diversity is a hallmark of developmental potential. *Science*. 2020;367:405-411.
6. Wilkinson AC, Nakauchi H, Gottgens B. Mammalian transcription factor networks: recent advances in interrogating biological complexity. *Cell Syst*. 2017;5(4):319-331. doi:10.1016/j.cels.2017.07.004
7. Osterwalder M, Tran T, Hunter R, et al. Characterization of mammalian in vivo enhancers using mouse transgenesis and

CRISPR genome editing. In: Walker JM, ed. *Craniofacial Development Methods in Molecular Biology*. Humana Press; 2022.
8. Osterwalder M, Barozzi I, Tissieres V, et al. Enhancer redundancy provides phenotypic robustness in mammalian development. *Nature*. 2018;554(7691):239-243. doi:10.1038/nature25461
9. van Ouwerkerk AF, Bosada FM, Liu J, et al. Identification of functional variant enhancers associated with atrial fibrillation. *Circ Res*. 2020;127(2):229-243. doi:10.1161/CIRCRESAHA.119.316006
10. Vincentz JW, Firulli BA, Toolan KP, et al. Variation in a left ventricle-specific Hand1 enhancer impairs GATA transcription factor binding and disrupts conduction system development and function. *Circ Res*. 2019;125:575-589. doi:10.1161/CIRCRESAHA.119.315313
11. Yanagisawa H, Clouthier DE, Richardson JA, Charite J, Olson EN. Targeted deletion of a branchial arch-specific enhancer reveals a role of dHAND in craniofacial development. *Development*. 2003;130(6):1069-1078. doi:10.1242/dev.00337
12. Charite J, McFadden DG, Merlo G, et al. Role of Dlx6 in regulation of an endothelin-1-dependent, dHAND branchial arch enhancer. *Genes Dev*. 2001;15(22):3039-3049.
13. McFadden DG, Charite J, Richardson JA, Srivastava D, Firulli AB, Olson EN. A GATA-dependent right ventricular enhancer controls dHAND transcription in the developing heart. *Development*. 2000;127(24):5331-5341.
14. Massari ME, Murre C. Helix-loop-helix proteins: regulators of transcription in eucaryotic organisms. *Molec Cell Biol*. 2000;20(2):429-440.
15. Murre C. Helix–loop–helix proteins and the advent of cellular diversity: 30 years of discovery. *Genes Dev*. 2019;33:6-25. doi:10.1101/gad.320663
16. Firulli BA, Hadzic DB, McDaid JR, Firulli AB. The basic helix-loop-helix transcription factors dHAND and eHAND exhibit dimerization characteristics that suggest complex regulation of function. *J Biol Chem*. 2000;275(43):33567-33573.
17. Barnes RM, Firulli AB. A Twist of insight, the role of Twist-family bHLH factors in development. *Int J Dev Biol*. 2009;53(7):909-924.
18. van Dusen NJ, Firulli AB. Twist factor regulation of non-cardiomyocyte cell lineages in the developing heart. *Differentiation*. 2012;84(1):79-88. doi:10.1016/j.diff.2012.03.002
19. George RM, Guo S, Firulli BA, Rubart M, Firulli AB. Neonatal deletion of Hand1 and Hand2 within murine cardiac conduction system reveals a novel role for HAND2 in rhythm homeostasis. *J Cardiovasc Dev Dis*. 2022;9(7):1-14. doi:10.3390/jcdd9070214
20. Osterwalder M, Speziale D, Shoukry M, et al. HAND2 targets define a network of transcriptional regulators that compartmentalize the early limb bud mesenchyme. *Dev Cell*. 2014;31(3):345-357. doi:10.1016/j.devcel.2014.09.018
21. Vincentz JW, VanDusen NJ, Fleming AB, et al. A Phox2- and Hand2-dependent Hand1 cis-regulatory element reveals a unique gene dosage requirement for Hand2 during sympathetic neurogenesis. *J Neuro Sci*. 2012;32(6):2110-2120.
22. Galli A, Robay D, Osterwalder M, et al. Distinct roles of Hand2 in initiating polarity and posterior Shh expression during the onset of mouse limb bud development. *PLoS Genet*. 2010;6(4):e1000901. doi:10.1371/journal.pgen.1000901
23. Holler KL, Hendershot TJ, Troy SE, Vincentz JW, Firulli AB, Howard MJ. Targeted deletion of Hand2 in cardiac neural crest-derived cells influences cardiac gene expression and outflow tract development [research support, N.I.H., extramural]. *Dev Biol*. 2010;341(1):291-304.
24. Zhang Z, Sui P, Dong A, et al. Preaxial polydactyly: interactions among ETV, TWIST1 and HAND2 control anterior-posterior patterning of the limb. *Development*. 2010;137(20):3417-3426. doi:10.1242/dev.051789
25. Ruest L-B, Dager M, Yanagisawa H, et al. Dhand-cre transgenic mice reveal specific potential functions of dHAND during craniofacial development. *Dev Biol*. 2003;257(2):263-277. doi:10.1016/s0012-1606(03)00068-x
26. Srivastava D, Thomas T, Lin Q, Kirby ML, Brown D, Olson EN. Regulation of cardiac mesodermal and neural crest development by the bHLH transcription factor, dHAND. *Nat Genet*. 1997;16(2):154-160.
27. Barron F, Woods C, Kuhn K, Bishop J, Howard MJ, Clouthier DE. Downregulation of Dlx5 and Dlx6 expression by Hand2 is essential for initiation of tongue morphogenesis. *Development*. 2011;138(11):2249-2259.
28. Funato N, Chapman SL, McKee MD, et al. Hand2 controls osteoblast differentiation in the branchial arch by inhibiting DNA binding of Runx2. *Development*. 2009;136(4):615-625.
29. Clouthier DE, Garcia E, Schilling TF. Regulation of facial morphogenesis by endothelin signaling: insights from mice and fish. *Am J Med Genet A*. 2010;152A(12):2962-2973.
30. Funato N, Kokubo H, Nakamura M, Yanagisawa H, Saga Y. Specification of jaw identity by the Hand2 transcription factor. *Sci Rep*. 2016;6:28405. doi:10.1038/srep28405
31. Tsuchihashi T, Maeda J, Shin CH, et al. Hand2 function in second heart field progenitors is essential for cardiogenesis. *Dev Biol*. 2011;351(1):62-69.
32. te Welscher P, Fernandez-Teran M, Ros MA, Zeller R. Mutual genetic antagonism involving GLI3 and dHAND prepatterns the vertebrate limb bud mesenchyme prior to SHH signaling. *Genes Dev*. 2002;16(4):421-426.
33. Hopyan S. Biophysical regulation of early limb bud morphogenesis. *Dev Biol*. 2017;429(2):429-433. doi:10.1016/j.ydbio.2017.06.034
34. Petit F, Sears KE, Ahituv N. Limb development: a paradigm of gene regulation. *Nat Rev Genet*. 2017;18(4):245-258. doi:10.1038/nrg.2016.167
35. Corsi AK, Brodigan TM, Jorgensen EM, Krause M. Characterization of a dominant negative C. elegans Twist mutant protein with implications for human Saethre-Chotzen syndrome. *Development*. 2002;129(11):2761-2772. doi:10.1242/dev.129.11.2761
36. Firulli BA, Krawchuk D, Centonze VE, et al. Altered Twist1 and Hand2 dimerization is associated with Saethre-Chotzen syndrome and limb abnormalities. *Nat Genet*. 2005;37(4):373-381.
37. Delgado I, Giovinazzo G, Temino S, et al. Control of mouse limb initiation and antero-posterior patterning by Meis transcription factors. *Nat Commun*. 2021;12(1):3086. doi:10.1038/s41467-021-23373-9
38. Monti R, Barozzi I, Osterwalder M, et al. Limb-enhancer genie: an accessible resource of accurate enhancer predictions in the

developing limb. *PLoS Comput Biol*. 2017;13(8):e1005720. doi:10.1371/journal.pcbi.1005720
39. Ritter N, Ali T, Kopitchinski N, et al. The lncRNA locus handsdown regulates cardiac gene programs and is essential for early mouse development. *Dev Cell*. 2019;50:644-657.e8. doi:10.1016/j.devcel.2019.07.013
40. Barbosa AC, Funato N, Chapman S, et al. Hand transcription factors cooperatively regulate development of the distal midline mesenchyme. *Dev Biol*. 2007;310(1):154-168.
41. VanDusen NJ, Casanovas J, Vincentz Joshua W, et al. Hand2 is an essential regulator for two Notch-dependent functions within the embryonic endocardium. *Cell Rep*. 2014;9(6):2071-2083. doi:10.1016/j.celrep.2014.11.021
42. George RM, Firulli BA, Podicheti R, et al. Single cell evaluation of endocardial HAND2 gene regulatory networks reveals critical HAND2 dependent pathways impacting cardiac morphogenesis. *Development*. 2023;150:1-13. doi:10.1242/dev.201341
43. Anderson KM, Anderson DM, McAnally JR, Shelton JM, Bassel-Duby R, Olson EN. Transcription of the non-coding RNA upperhand controls Hand2 expression and heart development. *Nature*. 2016;539:433-436. doi:10.1038/nature20128
44. Consortium EP, Moore JE, Purcaro MJ, et al. Expanded encyclopaedias of DNA elements in the human and mouse genomes. *Nature*. 2020;583(7818):699-710. doi:10.1038/s41586-020-2493-4
45. Bonev B, Mendelson Cohen N, Szabo Q, et al. Multiscale 3D genome rewiring during mouse neural development. *Cell*. 2017;171(3):557-572 e24. doi:10.1016/j.cell.2017.09.043
46. Kothary R, Clapoff S, Darling S, Perry MD, Moran LA, Rossant J. Inducible expression of an hsp68-lacZ hybrid gene in transgenic mice. *Development*. 1989;105(4):707-714.
47. Kuhlbrodt K, Herbarth B, Sock E, Hermans-Borgmeyer I, Wegner M. Sox10, a novel transcriptional modulator in glial cells. *J Neuro Sci*. 1998;18(1):237-250.
48. Vincentz JW, Firulli BA, Lin A, Spicer DB, Howard MJ, Firulli AB. Twist1 controls a cell specification switch governing cell fate decisions within the cardiac neural crest. *PLoS Genet*. 2013;9(3):e1003405.
49. Hendershot TJ, Liu H, Sarkar AA, et al. Expression of Hand2 is sufficient for neurogenesis and cell type-specific gene expression in the enteric nervous system [research support, N.I.H., extramural research support, non-U.S. Gov't]. *Dev Dyn*. 2007;236(1):93-105.
50. Reichenbach B, Delalande JM, Kolmogorova E, et al. Endoderm-derived sonic hedgehog and mesoderm Hand2 expression are required for enteric nervous system development in zebrafish. *Dev Biol*. 2008;318(1):52-64. doi:10.1016/j.ydbio.2008.02.061
51. Lei J, Howard MJ. Targeted deletion of Hand2 in enteric neural precursor cells affects its functions in neurogenesis, neurotransmitter specification and gangliogenesis, causing functional aganglionosis. *Development*. 2011;138(21):4789-4800. doi:10.1242/dev.060053
52. Hendershot TJ, Liu H, Clouthier DE, et al. Conditional deletion of Hand2 reveals critical functions in neurogenesis and cell type-specific gene expression for development of neural crest-derived noradrenergic sympathetic ganglion neurons. *Dev Biol*. 2008;319(2):179-191.
53. Howard MJ, Stanke M, Schneider C, Wu X, Rohrer H. The transcription factor dHAND is a downstream effector of BMPs in sympathetic neuron specification. *Development*. 2000;127(18):4073-4081.
54. Vincentz JW, Firulli BA, Toolan KP, Osterwalder M, Pennacchio LA, Firulli AB. HAND transcription factors cooperatively specify the aorta and pulmonary trunk. *Dev Biol*. 2024;476:1-10. doi:10.1016/j.ydbio.2021.03.011
55. Li L, Miano JM, Cserjesi P, Olson EN. SM22 alpha, a marker of adult smooth muscle, is expressed in multiple myogenic lineages during embryogenesis. *Circ Res*. 1996;78(2):188-195.
56. Potthoff MJ, Olson EN. MEF2: a central regulator of diverse developmental programs. *Development*. 2007;134(23):4131-4140. doi:10.1242/dev.008367
57. Washkowitz AJ, Gavrilov S, Begum S, Papaioannou VE. Diverse functional networks of Tbx3 in development and disease. *Wiley Interdiscip Rev Syst Biol Med*. 2012;4(3):273-283. doi:10.1002/wsbm.1162
58. Rallis C, Del Buono J, Logan MP. Tbx3 can alter limb position along the rostrocaudal axis of the developing embryo. *Development*. 2005;132(8):1961-1970. doi:10.1242/dev.01787
59. Mori AD, Bruneau BG. TBX5 mutations and congenital heart disease: Holt-Oram syndrome revealed. *Curr Opin Cardiol*. 2004;19(3):211-215.
60. Lewandowski JP, Du F, Zhang S, et al. Spatiotemporal regulation of GLI target genes in the mammalian limb bud. *Dev Biol*. 2015;406(1):92-103. doi:10.1016/j.ydbio.2015.07.022
61. Baldarelli RM, Smith CM, Finger JH, et al. The mouse gene expression database (GXD): 2021 update. *Nucleic Acids Res*. 2021;49(D1):D924-D931. doi:10.1093/nar/gkaa914
62. Gray PA, Hui F, Luo P, et al. Mouse brain organization revealed through direct genome-scale TF expression analysis. *Science*. 2004;306:2255-2257.
63. Richardson L, Venkataraman S, Stevenson P, et al. EMAGE mouse embryo spatial gene expression database: 2014 update. *Nucleic Acids Res*. 2014;42:D835-D844. doi:10.1093/nar/gkt1155
64. Yokoyama S, Ito Y, Ueno-Kudoh H, et al. A systems approach reveals that the myogenesis genome network is regulated by the transcriptional repressor RP58. *Dev Cell*. 2009;17(6):836-848. doi:10.1016/j.devcel.2009.10.011
65. Rodriguez-Carballo E, Lopez-Delisle L, Zhan Y, et al. The HoxD cluster is a dynamic and resilient TAD boundary controlling the segregation of antagonistic regulatory landscapes. *Genes Dev*. 2017;31(22):2264-2281. doi:10.1101/gad.307769.117
66. Kim TH, Shivdasani RA. Stomach development, stem cells and disease. *Development*. 2016;143(4):554-565. doi:10.1242/dev.124891
67. McCracken KW, Wells JM. Mechanisms of embryonic stomach development. *Semin Cell Dev Biol*. 2017;66:36-42. doi:10.1016/j.semcdb.2017.02.004
68. Xu H, Firulli AB, Wu X, Zhang X, Howard MJ. HAND2 synergistically enhances transcription of dopamine-B-hydroxylase in the presence of Phox2a. *Dev Biol*. 2003;262:183-193.
69. Firulli AB. A HANDful of questions: the molecular biology of the HAND-subclass of basic helix-loop-helix transcription factors. *Gene*. 2003;312C:27-40.
70. Howard MJ. Mechanisms and perspectives on differentiation of autonomic neurons. *Dev Biol*. 2005;277(2):271-286.

71. Chen L, Fish AE, Capra JA. Prediction of gene regulatory enhancers across species reveals evolutionarily conserved sequence properties. *PLoS Comput Biol*. 2018;14(10):e1006484. doi:10.1371/journal.pcbi.1006484
72. Frank CL, Liu F, Wijayatunge R, et al. Regulation of chromatin accessibility and Zic binding at enhancers in the developing cerebellum. *Nat Neurosci*. 2015;18(5):647-656. doi:10.1038/nn.3995
73. Mannion BJ, Osterwalder M, Tran S, et al. Uncovering hidden enhancers through unbiased in vivo testing. *bioRxiv*. 2022. doi:10.1101/2022.05.29.493901
74. Goode DK, Callaway HA, Cerda GA, Lewis KE, Elgar G. Minor change, major difference: divergent functions of highly conserved cis-regulatory elements subsequent to whole genome duplication events. *Development*. 2011;138(5):879-884. doi:10.1242/dev.055996
75. Zeller R, Lopez-Rios J, Zuniga A. Vertebrate limb bud development: moving towards integrative analysis of organogenesis. *Nat Rev Genet*. 2009;10(12):845-858. doi:10.1038/nrg2681
76. Cretekos CJ, Wang Y, Green ED, Martin JF, Rasweiler JJ, Behringer RR. Regulatory divergence modifies limb length between mammals. *Genes Dev*. 2008;22(2):141-151. doi:10.1101/gad.1620408
77. Leal F, Cohn MJ. Loss and Re-emergence of legs in snakes by modular evolution of sonic hedgehog and HOXD enhancers. *Curr Biol*. 2016;26(21):2966-2973. doi:10.1016/j.cub.2016.09.020
78. Kvon EZ, Kamneva OK, Melo US, et al. Progressive loss of function in a limb enhancer during Snake evolution. *Cell*. 2016;167(3):633-642 e11. doi:10.1016/j.cell.2016.09.028
79. Infante CR, Mihala AG, Park S, et al. Shared enhancer activity in the limbs and phallus and functional divergence of a limb-genital cis-regulatory element in snakes. *Dev Cell*. 2015;35(1):107-119. doi:10.1016/j.devcel.2015.09.003
80. Ertzer R, Muller F, Hadzhiev Y, et al. Cooperation of sonic hedgehog enhancers in midline expression. *Dev Biol*. 2007;301(2):578-589. doi:10.1016/j.ydbio.2006.11.004
81. Firulli AB, McFadden DG, Lin Q, Srivastava D, Olson EN. Heart and extra-embryonic mesodermal defects in mouse embryos lacking the bHLH transcription factor Hand1. *Nat Genet*. 1998;18(3):266-270.
82. Firulli BA, Toolan KP, Harkin J, Millar H, Pineda S, Firulli AB. The HAND1 frameshift A126FS mutation does not cause hypoplastic left heart syndrome in mice. *Cardiovasc Res*. 2017;113:1732-1742. doi:10.1093/cvr/cvx166
83. Firulli BA, Fuchs RK, Vincentz JW, Clouthier DE, Firulli AB. Hand1 phosphoregulation within the distal arch neural crest is essential for craniofacial morphogenesis. *Development*. 2014;141(15):3050-3061. doi:10.1242/dev.107680
84. Barnes RM, Firulli BA, VanDusen NJ, et al. Hand2 loss-of-function in Hand1-expressing cells reveals distinct roles in epicardial and coronary vessel development. *Circ Res*. 2011;15(108):940-949.
85. Li L, Miano JM, Mercer B, Olson EN. Expression of the SM22alpha promoter in transgenic mice provides evidence for distinct transcriptional regulatory programs in vascular and visceral smooth muscle cells. *J Cell Biol*. 1996;132(5):849-859.
86. Abdennur N, Mirny LA. Cooler: scalable storage for Hi-C data and other genomically labeled arrays. *Bioinformatics*. 2020;36(1):311-316. doi:10.1093/bioinformatics/btz540
87. Lopez-Delisle L, Rabbani L, Wolff J, et al. pyGenomeTracks: reproducible plots for multivariate genomic datasets. *Bioinformatics*. 2021;37(3):422-423. doi:10.1093/bioinformatics/btaa692

How to cite this article: Ferguson CA, Firulli BA, Zoia M, Osterwalder M, Firulli AB. Identification and characterization of *Hand2* upstream genomic enhancers active in developing stomach and limbs. *Developmental Dynamics*. 2023;1-18. doi:10.1002/dvdy.646